

# Transient Absorption and Fluorescence Studies of Disstacking Phthalocyanine by Poly(ethylene oxide)

Zhenyu Sheng,<sup>†</sup> Xiaodong Ye,<sup>†</sup> Zhaoxiong Zheng,<sup>†</sup> Shuqin Yu,<sup>†</sup> Dennis K. P. Ng,<sup>‡</sup> To Ngai,<sup>‡</sup> and Chi Wu<sup>\*,†,‡</sup>

The Opening Laboratory for Bond-Selective Chemistry, Department of Chemical Physics, University of Science and Technology of China, Hefei, Anhui 230026, China, and Department of Chemistry, The Chinese University of Hong Kong, Shatin, N.T.; Hong Kong

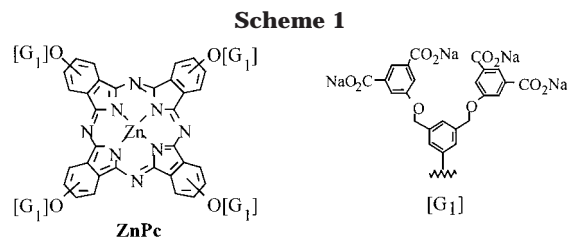
Received October 23, 2001; Revised Manuscript Received February 5, 2002

**ABSTRACT:** The interaction between phthalocyanine (ZnPc) and poly(ethylene oxide) (PEO) in water has been studied by dynamic laser light scattering and transient absorption and fluorescence spectroscopies. After the addition of PEO, the intensity of the transient absorption at ca. 490 nm, arising from the triplet state of the nonaggregated ZnPc, increases, and the triplet lifetime becomes longer. These results together with the fluorescence quenching experiments reveal that PEO behaves as a dispersion agent to disstack phthalocyanine macrocycles into individual molecules. It has been found that an equimolar amount of long PEO chains ( $M_w \sim 10\,000\text{ g mol}^{-1}$ ) can completely disstack ZnPc aggregates in water. A long PEO chain is about 8 times more effective than its short counterpart ( $M_w \sim 2000\text{ g mol}^{-1}$ ). The disstacking process has also been monitored by dynamic light scattering, which shows that the average particle size decreases significantly upon the addition of PEO. Since PEO is a FDA-certified biocompatible polymer material, such a phthalocyanine system has a potential application in photodynamic therapy.

## Introduction

Owing to their potential applications as photosensitizers in solar energy conversion<sup>1</sup> and photodynamic therapy,<sup>2</sup> phthalocyanines and their metal complexes have recently received considerable attention. One of the intrinsic problems of using these macrocycles is their strong stacking tendency to form dimer, trimer, and other aggregated species in solution.<sup>3</sup> This phenomenon is particularly serious in aqueous solutions because of strong hydrophobic interactions.<sup>4</sup> It has been found that such a stacking can lead to an efficient nonradioactive energy relaxation, reducing the triplet-state population and, consequently, significantly decreasing the photosensitizing efficacy.<sup>5</sup> Much effort in the past has therefore been put to generate nonaggregated phthalocyanines in aqueous media.

We have recently shown that four second-generation poly(aryl ether) dendritic fragments with terminal carboxylate moieties are sufficiently large to prevent the aggregation of a zinc(II) phthalocyanine core.<sup>6</sup> However, it is time-consuming and expensive to prepare high generation dendritic phthalocyanines. A simple and low-cost method has to be developed for a real application. For lower generation analogues, cationic surfactants such as hexadecyltrimethylammonium bromide are very effective to inhibit the stacking because of the electrostatic interaction between the anionic terminal groups of the dendritic fragments and the cationic heads of the surfactants.<sup>7</sup> However, the toxicity of surfactant is a potential problem in biomedical applications. Therefore, it is ideal to find a system containing a biocompatible and biodegradable dispersant to disstack phthalocyanine. Previously, we briefly investigated the effects of hydrophilic poly(ethylene oxide) (PEO) on the aggregation behavior of the first-generation dendritic phthalocyanine (ZnPc, Scheme 1).<sup>8</sup>



Our preliminary results showed that long PEO chains have a potential in disstacking ZnPc, resulting in monomeric species. Here, we report a detailed study on such a system, focusing on the excited-state dynamics and the disstacking mechanism, using a combination of dynamic laser light scattering and transient absorption and fluorescence spectroscopies.

## Experimental Section

**Sample Preparation.** The synthesis of the first-generation dendritic phthalocyanine ZnPc was reported previously.<sup>6</sup> Two poly(ethylene oxide) (PEO) samples (from Aldrich with  $M_w = 2000$  and  $10\,000\text{ g mol}^{-1}$ ), denoted as PEO2000 and PEO10000, were used as received. Mixtures of ZnPc and PEO were prepared by adding aqueous solutions of ZnPc dropwise into PEO aqueous solutions under stirring. The resulting mixtures were bubbled with high-purity nitrogen (99.99%) for 20 min before the spectroscopic measurements. Triply distilled water was used as the solvent, and all the spectra were recorded at ambient temperature.

**Laser Flash Photolysis and Fluorescence Studies.** The instrumentation and experimental procedures used for laser flash photolysis were reported previously.<sup>9</sup> The excitation light was the third harmonic (355 nm) of a Nd:YAG laser (Spectra Physics, GCR-170, repetition rate of 10 Hz) with a duration of 8 ns. The analyzing light was from a 500 W xenon lamp. The laser and analyzing light beams perpendicularly passed through a quartz cell with an optical path length of 10 mm. A monochromator (MC-30N, Ritsu Oyo Kogaku) equipped with a GDB 59 photomultiplier at the rear of the exit slit was used to analyze the absorption. The signal from the photomultiplier

<sup>†</sup> University of Science and Technology of China.

<sup>‡</sup> The Chinese University of Hong Kong.

\* Corresponding author at The Hong Kong address.

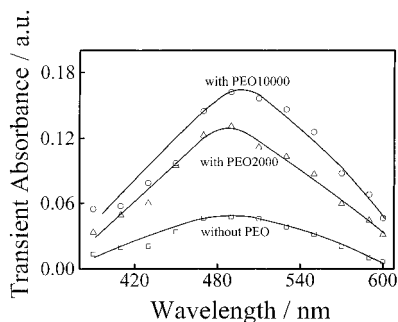


**Figure 1.** Transient absorption spectra of ZnPc in water with and without the addition of poly(ethylene oxide) after a 5  $\mu\text{s}$  irradiation ( $\lambda = 355 \text{ nm}$ ), where  $[\text{ZnPc}] = [\text{PEO10000}] = 0.2 \text{ mM}$ ,  $[\text{PEO2000}] = 1.0 \text{ mM}$ , and  $\text{pH} = 7.0$ . The transient absorption is defined as  $(I_0 - I)/I_0$  with  $I_0$  and  $I$  being the intensities of the transmitted light before and after the laser irradiation.

was instantly displayed and recorded on a Tektronix TDS 380 oscilloscope. Each data point was obtained by averaging the signals 256 times to improve the signal-to-noise ratio. The transient absorption spectra were obtained from a series of oscilloscope traces measured with the same solution in a point-by-point manner with respect to the wavelength. Fluorescence spectra were recorded on 970 CRT spectrophotometer.

**Dynamic Laser Light Scattering (LLS).** A commercial laser light scattering spectrometer (ALV/SP-125) equipped with an ALV-5000 multi- $\tau$  digital time correlator and an ADLAS DPY425II solid-state laser (output power = 400 mW at  $\lambda = 532 \text{ nm}$ ) was used. The Laplace inversion of each precisely measured intensity–intensity time correlation function  $G^{(2)}(t, q)$  in the self-beating mode resulted in a line width distribution  $G(\Gamma)$ . In this study, the CONTIN Laplace inversion algorithm in the correlator was used. For a pure diffusive relaxation,  $G(\Gamma)$  can be converted to a translation diffusion coefficient distribution  $G(D)$  by  $\Gamma = Dq^2$  or a hydrodynamic radius distribution  $f(R_h)$  using the Stokes–Einstein equation. The ZnPc/PEO mixtures were clarified with 0.2  $\mu\text{m}$  Millipore filters to remove dust. All the LLS measurements were done at  $25.0 \pm 0.1 \text{ }^\circ\text{C}$ . The details of the LLS instrumentation and theory can be found elsewhere.<sup>10</sup>

## Results and Discussion

It is well-known that non- $\alpha$ -substituted zinc(II) phthalocyanines show typical absorptions at ca. 350 and 680 nm, which can be attributed to the B (or Soret)-band and the Q-band, respectively, both arising from a  $\pi$ - $\pi^*$  transition.<sup>11</sup> A weak vibronic band at ca. 620 nm may also appear. For aggregated species, the Q-band is usually broadened and blue-shifted to ca. 650 nm.<sup>4</sup> As reported previously, a monomer-like absorption spectrum can be obtained for ZnPc upon addition of PEO.<sup>8</sup> A strong fluorescence emission at ca. 700 nm due to the monomeric species can also be observed. Upon excitation with a 5  $\mu\text{s}$  pulse laser at 355 nm, a transient absorption band at ca. 490 nm was detected, and its intensity increased upon the addition of PEO (Figure 1). For a given PEO molar concentration, the increment was more pronounced when longer PEO chains were used.

Figure 2 shows the decay of the transient absorption at 490 nm for ZnPc/PEO10000 aqueous solutions that have been purged with air or nitrogen for 20 min. It can be seen that, without prior purging of nitrogen, the decay process was extremely fast. This suggests that oxygen in air according to Scheme 2 can quench the excited state of ZnPc. The transient absorption at ca. 490 nm is therefore attributed to the excited triplet state of nonaggregated ZnPc. Since the concentration of the ground state of ZnPc can be regarded as a constant, the

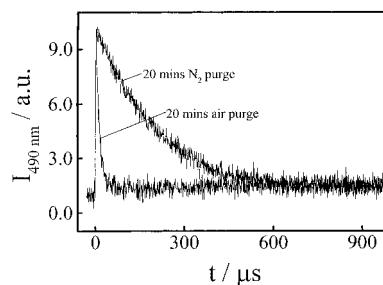


**Figure 2.** Time dependence of transient absorption intensity at 490 nm, where  $[\text{ZnPc}] = [\text{PEO10000}] = 0.2 \text{ mM}$ .

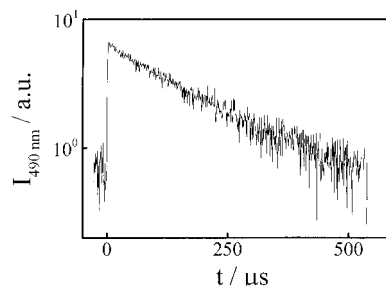


**Figure 3.** A semilogarithmic plot of time dependence of transient absorption intensity at 490 nm, where  $[\text{ZnPc}] = [\text{PEO10000}] = 0.3 \text{ mM}$  and the initial slope leads to a decay rate ( $1/\tau_T$ ).

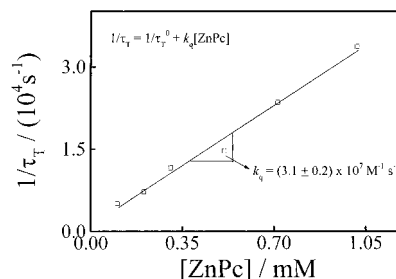
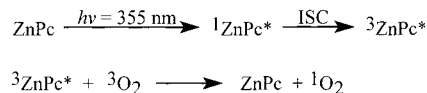


**Figure 4.** Concentration dependence of decay rate of transient absorption at 490 nm, where  $[\text{ZnPc}] = 0.2 \text{ mM}$  and  $\text{pH} = 7.0$ .

### Scheme 2



decay of  ${}^3\text{ZnPc}^*$  follows a pseudo-first-order kinetics. The initial slope of  $\log(I_{490 \text{ nm}})$  vs time leads to the characteristic quenching time  $\tau_T$  of the excited triplet state  ${}^3\text{ZnPc}^*$  (Figure 3). For a given PEO concentration,  $1/\tau_T$  can be related to the intrinsic excited triplet lifetime ( $\tau_T^0$ ) and the concentration of ZnPc as

$$1/\tau_T = 1/\tau_T^0 + k_q[\text{ZnPc}] \quad (1)$$

where  $k_q$  is the self-quenching rate constant for  ${}^3\text{ZnPc}^* + \text{ZnPc} \rightarrow 2\text{ZnPc}$ . Figure 4 shows a plot of  $1/\tau_T$  vs the ZnPc concentration, from which  $k_q$  was determined to be  $3.1 \times 10^7 \text{ M}^{-1} \text{ s}^{-1}$ . The small value of  $k_q$  indicates that the ground state of ZnPc is a weak quencher for  ${}^3\text{ZnPc}^*$ ; i.e., there exists a self-quenching process.

Figure 5 shows that for a given ZnPc concentration the PEO concentration affects not only the characteristic quenching time  $\tau_T$  but also the initial transient absorption  $\Delta I_{490 \text{ nm}}$ , defined as  $I_{490 \text{ nm}}$  (at  $t = t_0$  when the concentration of  ${}^3\text{ZnPc}^*$  reaches the maximum)  $- I_{490 \text{ nm}}$  (at  $t = \infty$ ). The PEO concentration dependences of  $\tau_T$

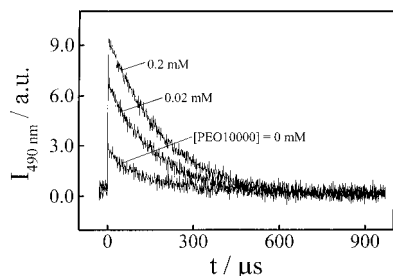


**Figure 5.** Time dependence of transient absorption intensity at 490 nm for different amounts of PEO10000 added, where  $[\text{ZnPc}] = 0.1 \text{ mM}$ .

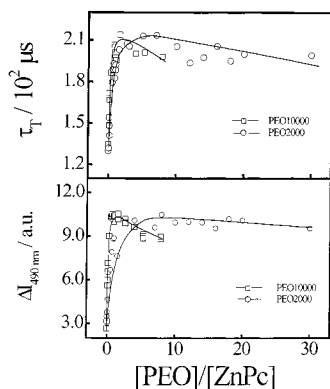


**Figure 6.** PEO concentration dependence of triplet lifetime and transient absorption at 490 nm, where  $[\text{ZnPc}]$  was kept at  $0.2 \text{ mM}$ .

and  $\Delta I_{490 \text{ nm}}$  are shown in Figure 6. It is clear that for a given  $\text{ZnPc}$  concentration both  $\tau_T$  and  $\Delta I_{490 \text{ nm}}$  increase with the PEO concentration. For long PEO chain (PEO10000), both  $\Delta I_{490 \text{ nm}}$  and  $\tau_T$  reach their corresponding maxima at  $[\text{PEO}]/[\text{ZnPc}] \sim 1$ , while the maxima occur at  $[\text{PEO}]/[\text{ZnPc}] \sim 8$  for short PEO chains (PEO2000). The increase in the transient absorption and the slowdown of the relaxation can be attributed to the disstacking of  $\text{ZnPc}$  aggregates and the disaggregation of the ground state by PEO. It is believed that the wrapping of monomeric  $\text{ZnPc}$  by PEO can hinder the self-quenching process, leading to a longer  $\tau_T$  and hence a stronger transient absorption. Apparently, PEO10000 is about 8 times more effective than PEO2000 in disstacking  $\text{ZnPc}$ . However, in terms of the weight concentration, PEO10000 is only ca. 1.6 times more effective as it is 5 times longer than PEO2000.

When  $\Delta I_{490 \text{ nm}}$  and  $\tau_T$  reach their corresponding maxima, we can assume that all  $\text{ZnPc}$  aggregates are disstacked into individual  $\text{ZnPc}$  molecules. Therefore, by taking  $\Delta I_{490 \text{ nm}}$  at the maximum as a 100% disstacking, we could estimate the monomer content  $[\text{ZnPc}]$  at different PEO concentrations, as shown in Figure 7. We found that  $\sim 30\%$  of  $\text{ZnPc}$  existed as individual molecules (monomers) even without PEO. The addition of PEO, in particular PEO10000, dramatically increased the monomer content. The slight decrease of  $\Delta I_{490 \text{ nm}}$ ,  $\tau_T$ , and  $X_{\text{monomer}}$  at high PEO concentrations, as shown in Figures 6 and 7, can be explained as follows. Assuming that a transition state  $^3(\text{ZnPc}-\text{ZnPc})^*$  arises after  $^3\text{ZnPc}^*$  and  $\text{ZnPc}$  collide with each other (Scheme 3), it can be derived that the overall reaction rate constant  $k$  is related to  $k_0 k_2 / (k_1 + k_2)$ . Without the addition of long PEO chains,  $k_2$  is much larger than  $k_1$ . Therefore,  $k \rightarrow k_0$  and  $k$  approaches the rate constant of the self-quenching in Figure 4. In the presence of PEO, two  $\text{ZnPc}$

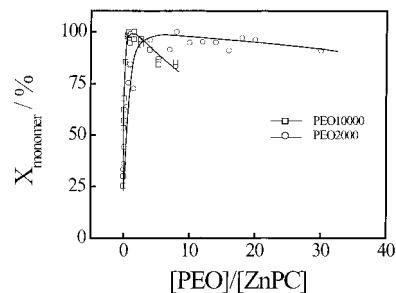


**Figure 7.** PEO concentration dependence of monomer content ( $X_{\text{monomer}}$ ) in an aqueous solution of  $\text{ZnPc}$ , where  $[\text{ZnPc}] = 0.2 \text{ mM}$ .

### Scheme 3

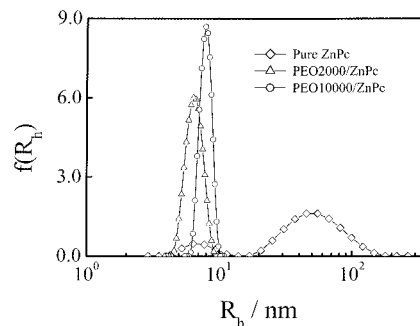
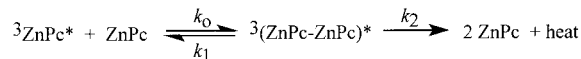


**Figure 8.** Hydrodynamic radius distributions  $f(R_h)$  of PEO/ $\text{ZnPc}$  complexes in water, where  $[\text{ZnPc}] = 0.1 \text{ mM}$  and  $[\text{PEO}]/[\text{ZnPc}] = 5.0$ .

monomers wrapped with long PEO chains have a less chance to approach each other so that  $k_0$  decreases, resulting in a smaller  $k$ . On the other hand, the addition of PEO increases the viscosity of the mixture and slows down the diffusion and collision, so that  $k_0$  decreases, but it has less effect on either  $k_1$  or  $k_2$ . After a complete disstacking of  $\text{ZnPc}$  aggregates, further addition of PEO could only lead to a possible "depletion"-induced flocculation,<sup>12</sup> resulting in an increase in  $k_0$ .

The disstacking of  $\text{ZnPc}$  by PEO can also be monitored by dynamic laser light scattering in terms of the change in average hydrodynamic radius ( $\langle R_h \rangle$ ). Figure 8 shows typical hydrodynamic radius distributions  $f(R_h)$  of PEO/ $\text{ZnPc}$  complexes. It is clear that, in the absence of PEO, the hydrodynamic radius distribution of  $\text{ZnPc}$  in water has two peaks, indicating that there exist two kinds of aggregates with different sizes. The peak located at  $\sim 7 \text{ nm}$  can be attributed to the dimers of  $\text{ZnPc}$ , which is a common form for aggregated phthalocyanines as a result of the face-to-face stacking.<sup>3,4,13</sup> The larger peak can be ascribed to the aggregation of many  $\text{ZnPc}$  molecules. The aggregation reveals that the first generation dendritic fragment is too small to disstack  $\text{ZnPc}$  into individual molecules. As shown in Figure 8, the addition of PEO clearly "dissolves" the aggregates, resulting in smaller particles, presumably individual PEO-wrapped  $\text{ZnPc}$  molecules.

To further demonstrate that the wrapping of  $\text{ZnPc}$  by PEO can retard the quenching of the excited states, we studied the interactions of  $\text{ZnPc}/\text{PEO}$  mixtures with potassium iodide (KI), which acts as a quencher. Figure 9 shows that the addition of KI to  $\text{ZnPc}/\text{PEO10000}$  decreases  $I_{490 \text{ nm}}(t_0)$  and speeds up the relaxation. The inset in Figure 9 reveals that in the presence of KI the

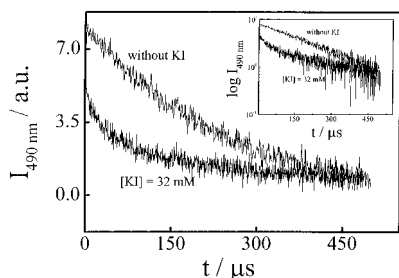


**Figure 9.** Time dependence of transient absorption intensity at 490 nm of a ZnPc/PEO10000 solution mixture with and without the addition of KI, where  $[\text{ZnPc}] = [\text{PEO10000}] = 0.2$  mM. The inset shows a semilogarithmic plot.

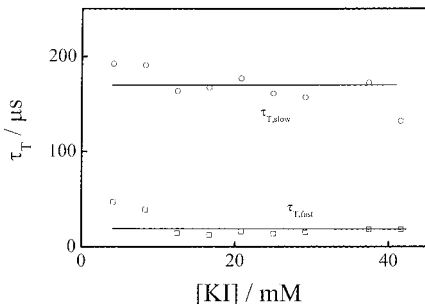


**Figure 10.** KI concentration dependence of lifetimes of fast and slow relaxations determined in Figure 9, where  $[\text{ZnPc}] = [\text{PEO10000}] = 0.2$  mM.

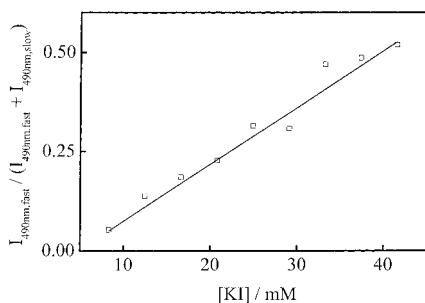


**Figure 11.** KI concentration dependence of contribution from fast component, where  $[\text{ZnPc}] = [\text{PEO10000}] = 0.2$  mM.

relaxation of the excited triplet state does not follow pseudo-first-order kinetics. The relaxation actually comprises two processes. To fit such a relaxation, we used a double-exponential fitting expressed as

$$I_{490 \text{ nm}}(t) = I_{490 \text{ nm,fast}} \exp\left(-\frac{t}{\tau_{T,\text{fast}}}\right) + I_{490 \text{ nm,slow}} \exp\left(-\frac{t}{\tau_{T,\text{slow}}}\right) \quad (2)$$

where  $\tau_{T,\text{fast}}$  and  $\tau_{T,\text{slow}}$  are the characteristic relaxation times of the  $\text{I}^-$ -induced quenching and the self-quenching of ZnPc, respectively, and  $I_{490 \text{ nm,fast}}(t_0) + I_{490 \text{ nm,slow}}(t_0) = I_{490 \text{ nm}}(t_0)$ .

Figure 10 shows the KI concentration dependence of  $\tau_{T,\text{fast}}$  and  $\tau_{T,\text{slow}}$ . As expected, both  $\tau_{T,\text{fast}}$  and  $\tau_{T,\text{slow}}$  are nearly independent of the KI concentration. It is worth noting that  $\tau_{T,\text{slow}}$  is close to  $\tau_T$  of ZnPc in solutions in the absence of KI (as shown in Figure 6). It confirms that the slow process is indeed related to the self-quenching. The  $\text{I}^-$ -induced quenching is  $\sim 10$  times faster than the self-quenching. Figure 11 shows that the contribution of the fast process increases linearly with the KI concentration. This further confirms that the fast

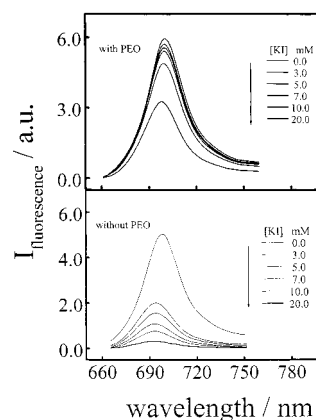


**Figure 12.** KI concentration dependence of emission spectra of ZnPc in water with and without the addition of PEO10000, where  $[\text{ZnPc}] = [\text{PEO10000}] = 0.1$  mM and  $\lambda_{\text{excitation}} = 617$  nm.

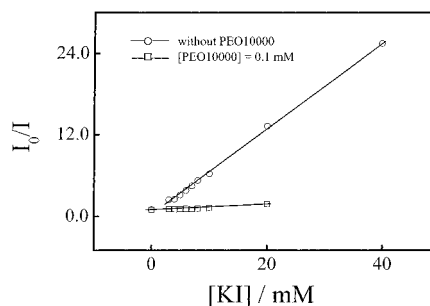


**Figure 13.** Stern–Volmer plots for KI-quenched fluorescence of ZnPc in water with and without the addition of PEO10000, where  $[\text{ZnPc}] = [\text{PEO10000}] = 0.1$  mM.

process is related to the  $\text{I}^-$ -induced quenching. A combination of Figures 9 and 10 shows that both of these quenching processes are intrinsic and not related to the collision frequency, which only affects their relative contributions to the total absorption.

The disstacking effect of PEO on ZnPc can also be viewed by fluorescence spectroscopy. Figure 12 shows that, in the presence of PEO, KI induces smaller effects on the fluorescence emission of ZnPc monomers. The results in Figure 12 could be analyzed by using the Stern–Volmer equation (eq 3),<sup>14</sup>

$$I_0/I = 1 + K_{\text{SV}}[\text{quencher}] \quad (3)$$

where  $I_0$  and  $I$  are the fluorescence intensities in the absence and presence of the quencher, respectively, and  $K_{\text{SV}}$  is the Stern–Volmer quenching constant. Figure 13 shows that the fluorescence intensities are well represented by the Stern–Volmer equation. The fittings lead to  $K_{\text{SV}} = (6.3 \pm 0.1) \times 10^2$  and  $42 \pm 4 \text{ mol}^{-1} \text{ dm}^3$  for the ZnPc aqueous solutions in the absence and presence of PEO, respectively. This shows that  $\text{I}^-$  is an effective quencher for the excited singlet state of ZnPc monomer, but PEO can reduce this quenching effect. The PEO chains therefore have dual functions, namely disstacking and wrapping. Taking the wrapping ratio in a pure ZnPc solution as zero, we could estimate the wrapping ratio in the presence of PEO10000 from the ratio of the two  $K_{\text{SV}}$  values. It shows that long PEO chains can wrap 94% of ZnPc monomers.

## Conclusions

Using transient absorption spectroscopy, dynamic laser light scattering, and fluorescence quenching meth-

ods, we have shown that PEO can disstack ZnPc aggregates effectively. The results of the triplet state transient absorption reveal that, for a given molar concentration, longer PEO10000 can disstack ZnPc 8 times more effectively than shorter PEO2000. The fluorescence quenching study further confirms that long PEO chains can entrap the macrocycles into individual molecules. Such a PEO/ZnPc system has a potential in biomedical and catalytic applications because PEO is a FDA-certified biocompatible and biodegradable polymer.

**Acknowledgment.** The financial support of this work by NKBRF, National Key Basic Research Special Found, and HKSAR RGC Earmarked Grants (CUHK4266/00p, 2160135; CUHK 4117/98P, 2160106) is gratefully acknowledged.

## References and Notes

- (1) See for example: (a) Wöhrle, D.; Kreienhoop, L.; Schlettwein, D. In *Phthalocyanines—Properties and Applications*; Leznoff, C. C., Lever, A. B. P., Eds.; VCH: New York, 1996; Vol. 4, pp 219–284. (b) Nazeeruddin, M. K.; Humphry-Baker, R.; Grätzel, M.; Murrer, B. A. *Chem. Commun.* **1998**, 719. (c) Nazeeruddin, M. K.; Humphry-Baker, R.; Grätzel, M.; Wöhrle, D.; Schnurpfeil, G.; Schneider, G.; Hirth, A.; Trombach, N. *J. Porphyrins Phthalocyanines* **1999**, 3, 230.
- (2) (a) Ali, H.; van Lier, J. E. *Chem. Rev.* **1999**, 99, 2379. (b) Lukyanets, E. A. *J. Porphyrins Phthalocyanines* **1999**, 3, 424. (c) Allen, C. M.; Sharman, W. M.; van Lier, J. E. *J. Porphyrins Phthalocyanines* **2001**, 5, 161.
- (3) Choi, M. T. M.; Li, P. P. S.; Ng, D. K. P. *Tetrahedron* **2000**, 56, 3881 and references therein.
- (4) (a) Schelly, Z. A.; Harward, D. J.; Hemmes, P.; Eyring, E. M. *J. Phys. Chem.* **1970**, 74, 3040. (b) Yang, Y.-C.; Ward, J. R.; Seiders, R. P. *Inorg. Chem.* **1985**, 24, 1765.
- (5) (a) Dhami, S.; Phillips, D. *J. Photochem. Photobiol. A: Chem.* **1996**, 100, 77. (b) Howe, L.; Zhang, J. Z. *J. Phys. Chem. A* **1997**, 101, 3207. (c) Fernandez, D. A.; Awruch, J.; Dicalio, L. E. *J. Photochem. Photobiol. B: Biol.* **1997**, 41, 227. (d) Lang, K.; Kubát, P.; Mosinger, J.; Wagnerová, D. M. *J. Photochem. Photobiol. A: Chem.* **1998**, 119, 47.
- (6) Ng, A. C. H.; Li, X.-y.; Ng, D. K. P. *Macromolecules* **1999**, 32, 5292.
- (7) Li, X.-y.; He, X.; Ng, A. C. H.; Wu, C.; Ng, D. K. P. *Macromolecules* **2000**, 33, 2119.
- (8) Ngai, T.; Zheng, G.-Z.; Li, X.-Y.; Ng, D. K. P.; Wu, C. *Langmuir* **2001**, 17, 1381.
- (9) Sheng, Z.-Y.; Song, Q.-H.; Yu, S.-Q. *Res. Chem. Intermed.* **2000**, 26, 715.
- (10) (a) Berne, B.; Pecora, R. *Dynamic Light Scattering*; Plenum Press: New York, 1976. (b) Chu, B. *Laser Light Scattering*, 2nd ed.; Academic Press: New York, 1991.
- (11) Stillman, M. J.; Nyokong, T. In *Phthalocyanines—Properties and Applications*; Leznoff, C. C., Lever, A. B. P., Eds.; VCH: New York, 1989; Vol. 1, Chapter 3.
- (12) Jenkins, P.; Snowden, M. *Adv. Colloid Interface Sci.* **1996**, 68, 57.
- (13) Kaneko, Y.; Arai, T.; Tokumaru, K.; Matsunaga, D. *Chem. Lett.* **1996**, 5, 345.
- (14) Winnik, M. A.; Bystryak, S. M.; Liu, Z.-Q.; Siddiq, J. *Macromolecules* **1998**, 31, 6885.

MA011838P